

STRATEGIES FOR OVERCOMING LIMITATIONS OF SULFUR DETERMINATION IN GEOLOGICAL SAMPLES BY WAVELENGTH DISPERSIVE X-RAY FLUORESCENCE SPECTROMETRY

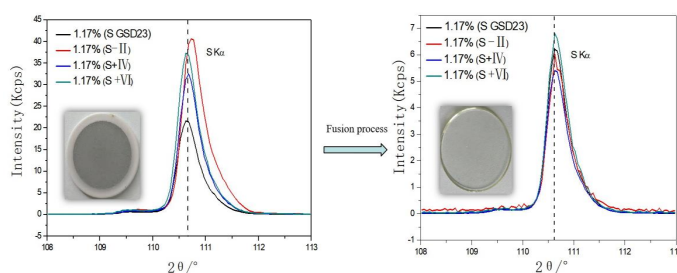
Jiu-Fen LIU,^a Wen-Zhi ZHAO,^{b*} Li-Ming XU,^b Ying-Zheng PEI^b and Xu XIE^b

^aCommand center for Natural Resources Comprehensive Survey, China Geological Survey, Beijing, 100010, P. R. China

^bCenter for Harbin Natural Resources Comprehensive Survey, China Geological Survey, Harbin, 150039, P. R. China

Received August 6, 2021

A new strategy for overcoming limitations of sulfur determination in geological samples by wavelength dispersive X-ray fluorescence spectroscopy (WD-XRF) was developed. A new way of preparing the beads has been established, adding the quantity of sulfur-fixing agent required for the sulfur contained in the sample to form a stable sulfate compound, which suppresses the problem of sulfur loss during the fusion process. Twenty-four geological reference samples were used to calibrate and evaluate the analytical method. The sulfur fixation effect of sulfur-fixing agent BaO was better than that of sulfur-fixing agent CaO, the addition of sulfur-fixing agent BaO can effectively improve the accuracy of the results and the trueness of the method validation samples was -9.0-5.7%, showing good accuracy. The results of WD-XRF, inductively coupled plasma emission spectroscopy (ICP-OES) and combustion-IR detection were compared. With reference to the quality standard assessment proposed by the IGCP, from which it can be deduced that the method was adequate considering geochemical mapping application.



INTRODUCTION

Sulfur is one of the important chemical elements in nature. Sulfur owns several inorganic species, and it has five valences including S -II, S 0, S +II, S +IV and S +VI.^{1,2} Sulfur is a non-metallic element that is routinely analyzed in geological samples, and it is also a must-test item in regional geological surveys.³ There are many determination methods for sulfur in geological samples. The traditional methods mainly include barium sulfate gravimetric method,⁴ spectrophotometric method, combustion volume method⁵ and tube furnace combustion. Modern instrumental determination methods include combustion-IR

detection,^{6,7} wavelength dispersive X-ray fluorescence spectroscopy (WD-XRF),^{8,9} inductively coupled plasma emission spectroscopy (ICP-OES)^{10,11} and ion chromatography (IC).^{12,13} X-ray fluorescence spectrometry has the advantages of simple sample preparation, fast detection speed, high analysis accuracy, environmental protection and simultaneous determination of major and minor elements, so it has a wide range of application prospects.¹⁴⁻¹⁶

However, there are few reports on the determination of sulfur in geological samples by WD-XRF. This is due to the large variety of sulfur-containing minerals, which seriously affects the accuracy of WD-XRF determination methods in

* Corresponding author: zhaowenzi817@163.com; Tel.: +86-451-86380079

complex geological samples.^{17,18} How to obtain accurate analysis values of sulfur using WD-XRF determination methods has become a major problem for analysts. In WD-XRF analysis, the geological samples need to be prepared in the form of beads or pellets.^{19,20} The use of pellets to analyze sulfur is faster, simpler, greener and more environmentally friendly, and can give full play to the advantages of WD-XRF. Mineral structure and matrix effects can seriously affect the accuracy, thus making it necessary to have calibration samples with the same mineral structure, particle size and chemical composition as the sample under study, which limits the application.²¹⁻²³ If the sample is prepared in the form of beads, the matrix effect can be effectively eliminated, but the high melting temperature will cause sulfur volatilization.²⁴

In this study, a new way of preparing the beads has been established to suppress the problem of sulfur loss during the fusion process. Samples were prepared in the form of beads to overcome mineral effect and particle size effect, in this procedure the required quantity of sulfur-fixing agent CaO and BaO was added respectively to combine with the sulfur present in the sample and form a stable CaSO₄ and BaSO₄ compounds respectively, thus eliminating the problem of sulfur loss during the

fusion process. In addition, method validation and comparison with ICP-OES and combustion-IR detection were also performed.

RESULTS AND DISCUSSION

1. Study on valence and matrix effects of sulfur by WD-XRF

Fig. 1 present the spectral lines and intensities obtained by monitoring the S K α in the form of pellets and beads, respectively. The three S species prepared using FeS, Na₂SO₃ or Na₂SO₄ diluted in Na₂CO₃, respectively. The S content in all species was consistent with GSD23, both with 1.17% S.

The diffraction angles (2θ) of S K α lines of different species in the form of pellets were different, as shown in Table 1, which indicated that the lines had shifted, and the difference values of 2θ were 0.09°. 2θ of S K α lines of different species in the form of beads were very close to that of sulfate, which indicates that by adding oxidant to melt, low-valence sulfur is converted into sulfate sulfur.

Table 1

The diffraction angles and fluorescence intensity of different inorganic sulfur species by WD-XRF

Species	Pellets (S K α)		Beads (S K α)	
	$2\theta/^\circ$	Peak (Kcps)	$2\theta/^\circ$	Peak (Kcps)
GSD23	110.675	21.631	100.660	6.208
Sulfide(S - II)	110.751	40.604	100.661	6.022
Sulphite(S + IV)	110.685	32.496	100.660	5.408
Sulphate(S + VI)	110.661	37.250	100.662	6.809

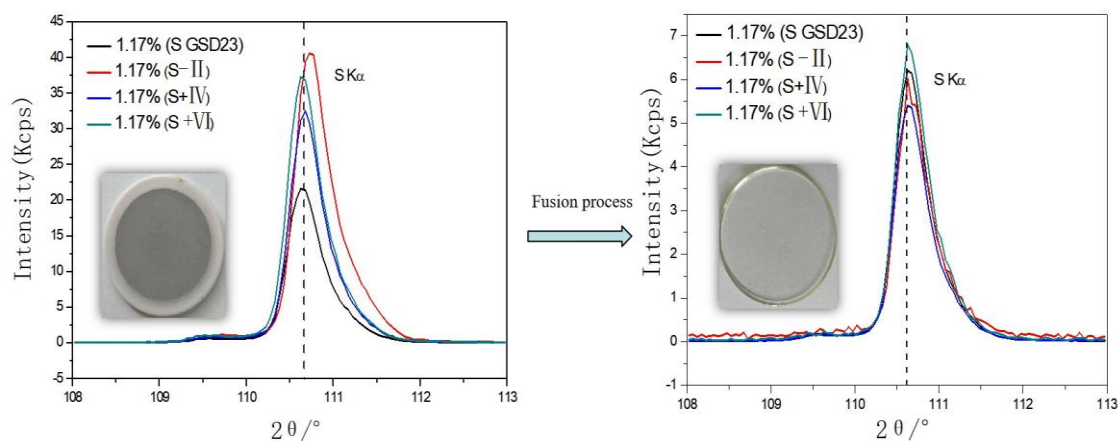


Fig. 1 – S K α spectra of different inorganic sulfur in the form of pellets and beads.

Matrix effect is one of the main errors in XRF analysis, especially for direct analysis in the form of pellets. Matrix effect is due to the change in characteristic X-ray intensity, caused by excitation (absorption) and scattering. As shown in Fig. 1 and Table 1, compared with the intensity of GSD23, the samples prepared with FeS, Na₂SO₃ and Na₂SO₄ in the form of pellets showed significant enhancement effect, approximately 1.9, 1.5 and 1.7 fold greater intensity than S K α of GSD23 line.

When the sample is prepared in the form of beads, sample is diluted to minimize the matrix effect, while the formation of fused glass discs eliminates the influence of the mineral structure. However, the high temperature of the fusion process may cause the loss of sulfur in the sample due to volatilization, which can be avoided by adding a sulfur-fixing agent to the sample

2. Preparation of the calibration curves

Sulfur was determined by WD-XRF spectrometry using the analytical line K α ($2\theta = 110.683^\circ$) with a 0.55 mm collimator and a Ge111 crystal, applying voltage/current of 25 kV/160 mA and a flow detector.

Because the fusion method was used to prepare the sample, the particle size effect and mineral

effect of the sample are eliminated, and the matrix effect of the sample was reduced. However, due to the different content of major and minor elements in geological samples, the theoretical α coefficient was still needed for the matrix effect and the empirical coefficient was used to correct the overlap of the spectral lines. The comprehensive mathematical correction formula was illustrated in Eq. (1):

$$\omega_i = D_i - \sum L_{im} R_m + k_i R_i (1 + \sum_{j \neq i}^N \alpha_{ij} \cdot \omega_j) \quad (1)$$

Where W is the mass fraction of analysis element i in the unknown sample, D_i is the intercept of the calibration curve, L_{im} is the interference correction coefficient of spectral line that overlap the analysis element i ; R_m is the count rate of the interference element m ; k_i is the slope of the calibration curve of the analysis element i ; R_i is the count rate of the analysis element i ; N is the number of coexisting elements; α is the factor to correct the matrix effect; i is the analysis element; j is the coexisting element.

The S K α line was used as the analysis line; the matrix correction elements were Ca, Fe, Si, Al, Na and K; the Mo L α line was subtracted to eliminate overlapping spectral lines.

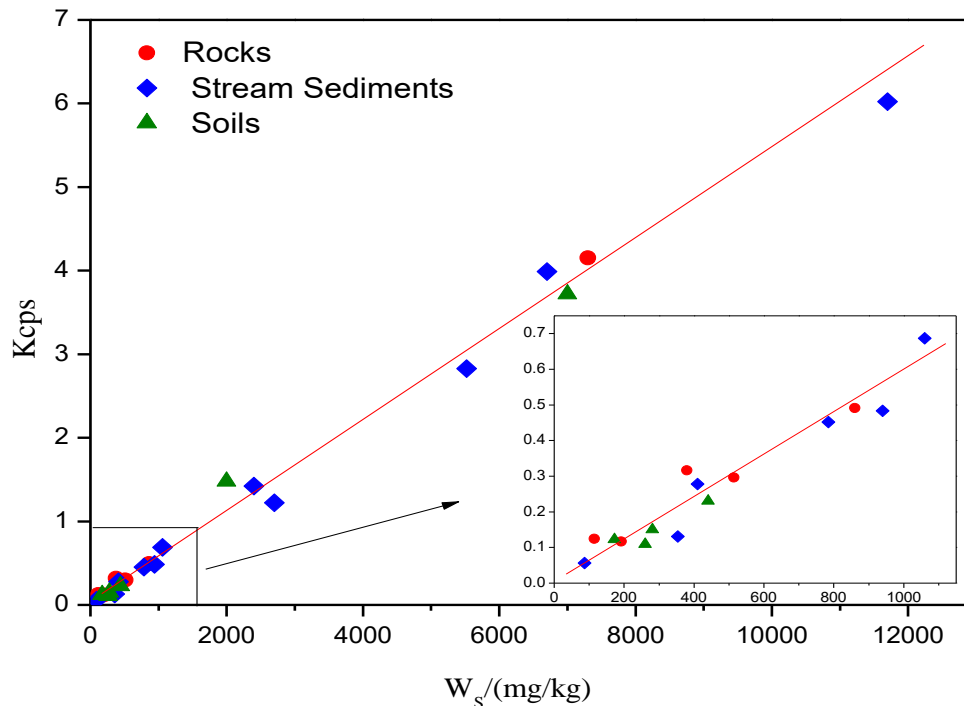


Fig. 2 – Calibration curve for sulfur with samples prepared in the form of beads without sulfur-fixing agent.

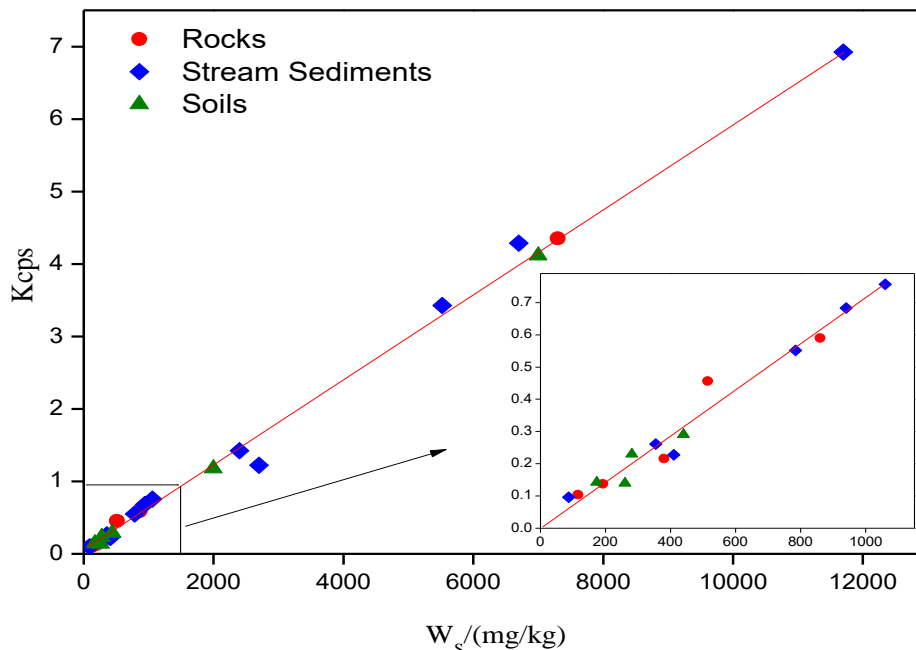


Fig. 3 – Calibration curve for sulfur with samples prepared in the form of beads with sulfur-fixing agent CaO addition.

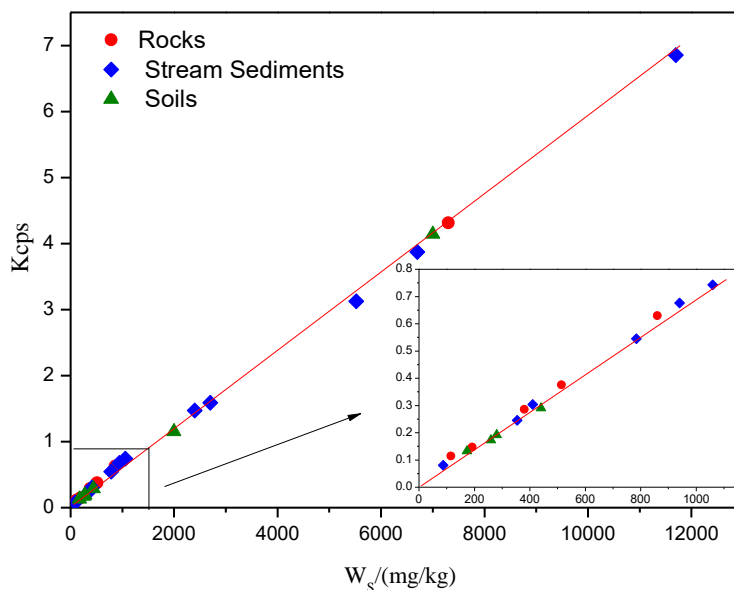


Fig. 4 – Calibration curve for sulfur with samples prepared in the form of beads with sulfur-fixing agent BaO addition.

Fig. 2-4 showed the calibration curves obtained when the samples were prepared in the form of beads without sulfur fixation sorbent, beads with sulfur-fixing agent CaO addition, and beads with sulfur-fixing agent BaO addition, respectively. Fig. 2 revealed a large data scatter, which corresponded to sample preparation in the form of beads without sulfur-fixing agent, possibly due to the loss of sulfur in the fusion process, so the curve cannot accurately determine the sulfur content in the sample. Fig. 3, which corresponded to sample

preparation in the form of beads with the addition of sulfur-fixing agent CaO, showed a better correlation than Fig. 2. However, there were still obvious data scatter points, which may be due to the high temperature decomposition of CaSO_4 to generate SO_2 , resulting in loss of sulfur. Fig. 4 showed a good correlation due to the suppression of mineral structure and matrix effects, and the formation of stable BaSO_4 due to the addition of sulfur-fixing agent BaO, which minimizes the loss of sulfur during preparation.

Table 2
Concentrations determined of sulfur in different inorganic sulfur species by WD-XRF

Sample	reference samples			FeS diluted in Na ₂ CO ₃			Na ₂ SO ₃ diluted in Na ₂ CO ₃			Na ₂ SO ₄ diluted in Na ₂ CO ₃								
	Certified (mg/kg)	Measured (mg/kg)	Trueness (%)	Reference value (mg/kg)	Measured (mg/kg)	Trueness (%)	Sample	Reference value (mg/kg)	Measured (mg/kg)	Trueness (%)	Sample	Reference value (mg/kg)	Measured (mg/kg)	Trueness (%)				
GSS2	210±43	204±4	-2.7	210	199±8	-5.1	S ² -1	210	199±8	-5.1	SO ₃ ²⁻ -1	210	214±3	2.0	SO ₄ ²⁻ -1	210	221±7	5.1
GSS32	77±9	76±2	-1.7	77	73±2	-5.3	S ² -2	77	73±2	-5.3	SO ₃ ²⁻ -2	77	73±1	-4.9	SO ₄ ²⁻ -2	77	81±1	5.7
GSD12	940±54	925±10	-1.6	940	955±27	1.5	S ² -3	940	955±27	1.5	SO ₃ ²⁻ -3	940	893±6	-5.0	SO ₄ ²⁻ -3	940	985±13	4.8
GSD23	11700±900	11072±107	-5.4	11700	11343±167	-3.1	S ² -4	11700	11343±167	-3.1	SO ₃ ²⁻ -4	11700	10648±186	-9.0	SO ₄ ²⁻ -4	11700	11560±226	-1.2

Measured values are for mean±confidence interval for an 95% confidence level of seven replicate measurements (n=7).

The detection limit used in WD-XRF analysis was calculated according the SUPER Q 5.0 analytical software,²⁵ using the Eqs. (2):

$$LOD = \frac{3}{m} \sqrt{\frac{I_b}{t_b}} \quad (2)$$

Where m is the unit content count rate, I_b is the background count rate, t_b is the background count time. After calculation, the LOD of the samples prepared in the form of beads without sulfur fixation sorbent, beads with sulfur-fixing agent CaO addition, and beads with sulfur-fixing agent BaO addition were 13.43 mg/kg, 13.57 mg/kg and 13.51 mg/kg, respectively. The LOD did not change significantly before and after adding sulfur-fixing agent.

3. Method validation

The proposed method was applied to determine sulfur in 16 samples containing different sulfur species, in which 4 samples were reference samples and the other 12 samples were prepared by using FeS, Na₂SO₃ and Na₂SO₄ diluted in Na₂CO₃. The samples were prepared in the form of beads with sulfur-fixing agent BaO to avoid sulfur loss.

The results were shown in Table 2. The reference value, the measured value and the trueness (%RE) were provided for each sample. The obtained values of the reference samples and the three sulfur compounds were very close to the reference value, the relative error (%RE) was adopted to evaluate the trueness of seven replicates of each sample, and their values was located in a range of -1.6~-5.4%, -5.3~1.5%, -9.0~2.0% and -1.2~5.7%, respectively, indicating a good accuracy. This result indicates that the sample was prepared in the form of beads for WD-XRD analysis of sulfur can significantly eliminate the matrix effect, and the addition of sulfur-fixing agent can effectively improve the accuracy of the results.

4. Comparison of accuracy and precision

In this work, 10 reference samples of soil, rocks and stream sediments were selected for the determination of S using WD-XRF, ICP-OES and combustion-IR detection. Each sample was independently measured 7 times by these three methods, and the measured value (n=7), the certified value, and trueness were obtained and illustrated in Table 3.

Table 3

Concentrations determined of S in reference samples by WD-XRF, ICP-OES and combustion-IR detection

Sample	Certified (mg/kg)	WD-XRF			ICP-OES			Combustion-IR detection		
		Measured (mg/kg)	Trueness (%)	RSD (%)	Measured (mg/kg)	Trueness (%)	RSD (%)	Measured (mg/kg)	Trueness (%)	RSD (%)
GSS2	210±43	207±4	-1.7	2.8	229±7	9.2	4	223±10	6.2	5.7
GSS24	2000±300	1913±53	-4.4	3.7	1967±59	-1.6	4.1	2188±70	9.4	4.3
GSS32	77±9	76±3	-1.5	5.4	81±1	5.7	2.3	74±6	-4.1	10.6
GSS34	431±22	392±7	-9	2.4	436±14	1.2	4.3	426±13	-1.2	3.9
GSD12	940±54	885±21	-5.9	3.1	922±33	-1.9	4.8	958±12	2	1.7
GSD23	11700±900	12040±215	2.9	2.4	12002±276	2.6	3.1	11313±318	-3.3	3.8
GSD27	1060±60	1126±42	6.2	5	1154±19	8.8	2.2	1023±21	-3.5	2.8
GSD28	5520±170	4973±87	-9.9	2.4	5256±77	-4.8	2	5670±142	2.7	3.4
GSR1	380±33	366±7	-3.7	2.5	371±6	-2.4	2.2	399±5	5	1.6
GSR16	(690)	697±14	1	2.7	713±23	3.4	4.4	713±7	3.4	1.4

Measured values are for mean±confidence interval for an 95% confidence level of seven replicate measurements (n=7); Values in parenthesis are reference value

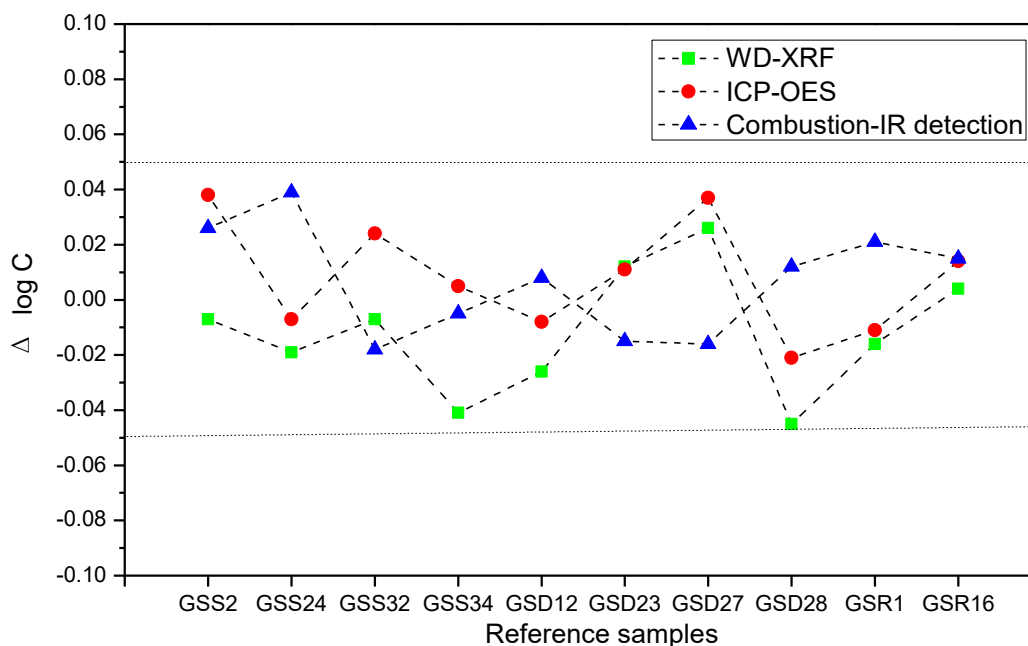


Fig. 5 – Test proposed by IGCP for accuracy evaluation in geochemical mapping. The dotted line is the quality control line.

All the trueness of sulfur determination were better than 9.9% for WD-XRF and better than 9.2% for ICP-OES and better than 9.4% for combustion-IR detection. This showed that the determination of S by WD-XRF in the form of beads with sulfur-fixing agent BaO displayed good trueness. Precision of seven replicates of each sample was expressed as the relative standard deviation (%RSD). The result in Table 3 indicated that for all samples the %RSD values were better than 10% by using WD-XRF and ICP-OES. WD-XRF and ICP-OES had similar precision, the RSD values were better than 5.4% and 4.8%, respectively, performing good precision. The values measured by combustion-IR detection fluctuated significantly, especially the values for low sulfur content, the value of GSS32 sample was 10.6%. Consequently, the WD-XRF method established in this work is an effective method for the determination of sulfur in geological samples.

In addition, the fitness for purpose of the results was also evaluated by the quality test proposed by the International Global Geochemical Mapping Program (IGCP),²⁶ which compares the differences between measured and certified values by the expression of $\Delta \log C$ ($\log C_s - \log C_i$), where C_s and C_i are the measured and certified value, respectively. According to IGCP standard, the reference samples measured in this work would be considered $\Delta \log C$ between ± 0.05 for S. **Fig. 5** was the plots obtained by performing the IGCP test to the results of sulfur by WD-XRF, ICP-OES and combustion-IR detection. The result indicates that

the accuracies of the three methods have similar accuracy, and all $\Delta \log C$ are between -0.05 and 0.05, performing acceptable accuracy. It can be deduced that considering the application of geochemical mapping, the method of determining S using WD-XRF is adequate.

EXPERIMENTAL

1. Instrument

The pellets were formed in a hydraulic press (BRE-33, maekawa, Japan). The beads were prepared for WD-XRF analysis in a automatic fusion bead machine (Eagon 2, PANalytical, The Netherlands). WD-XRF analysis was performed with a PANalytical Axios^{max} WD-XRF spectrometer with Rh-target tube, coupled with a PW 4400 automatic sample changer and provided with a SUPER Q 5.0 suitable software. Comparisons of S concentrations were obtained using an ICP-OES (iCAP 6000, Thermo Scientific, USA) and combustion-IR detection (COREY-205, KERUI, China). The optimized measuring conditions of the instruments were shown in Table 4.

2. Materials

The following reference materials were used for calibration in WD-XRF analysis: GSR1-2, GSR4, GSR18-20 (rocks, IGGE, China); GSD4-6, GSD12, GSD16, GSD21, GSD23, GSD27-28, GSD3a, GSD5a (stream sediments, IGGE, China); GSS6, GSS14, GSS18, GSS20, GSS22, GSS24, GSS28 (soil, IGGE, China); method validation and comparative experiments were carried out using the following reference samples: GSS2, GSS24, GSS32, GSS34 (soil, IGGE, China); GSD12, GSD23, GSD27, GSD28 (stream sediments, IGGE, China); GSR1, GSR16 (rocks, IGGE, China).

Table 4

Operating parameters of WD-XRF, ICP-OES and combustion-IR detection

WD-XRF		ICP-OES		Combustion-IR detection	
Item	Parameter	Item	Parameter	Item	Parameter
Line	K α	Pump rate	50 rpm	Temperature	25 °C
Crystal	Ge (111)	Nebulizer gas flow	0.6 L/min	Oxygen supply pressure	0.08 MP
Collimator	550 μ m	Centre tube	2.0 mm	Oxygen flow	2.5 L/min
Voltage	25 kV	RF forward power	1150 W	Cleaning time	30 s
Current	160 mA	Auxiliary flow	0.5 L/min	Heating time	25 s
2 θ (°)	110.679	Integration time	15 s UV / 10 s Vis	Analysis time	40 s
PHD1 LL	21	Emission line	S 182.034 nm		
PHD1 UL	79				
Detector	F-PC				

High purity water (18.2 M Ω cm resistivity) was obtained from GN-RO-500 Total Water System (Shuangfeng, Beijing, China). S standard solutions, containing 100 mg/L S, were used to prepare the ICP-OES calibration curve by the appropriate dilution of stock standard solution containing 1000 mg/L S (IGGE, China). CaO, BaO, HCl, HF, HClO₄, HNO₃, Na₂CO₃, FeS, Na₂SO₃ and Na₂SO₄ were all guaranteed reagent (Beijing Fuxing Chemical Industry Co. Ltd, China). Iron flux (purity>99.8%, particle size <1.25 mm,) and tungsten flux (20-40 mesh, purity \geq 99.95%) was supplied by Tiangang Co. Ltd, China.

3. Sample preparation in the form of beads

Accurately weigh 0.7000 g of the sample dried at 110°C in a porcelain crucible, and then weigh 7.0000 g of mixed flux (Li₂B₄O₇:LiBO₂=12:22). After stirring evenly with a wooden stick, moved it into a platinum crucible, added 2 ml of lithium nitrate solution and 2 drops of saturated lithium bromide solution, and oxidized at 600°C for 3 min, heated to 1100°C to melted for 10 min. Pour the melt into the mold, cooled and peeled off.

Beads were also prepared with and without the addition of as sulfur-fixing agent (CaO and BaO), adding a constant quantity of CaO and BaO in powder form to the foregoing ingredients (sample, flux, and release agent).

4. Sample preparation for total sulphur determinations by ICP-OES

0.2500 g of the sample was placed in a 50mL teflon beaker, 2.5 mL of nitric acid, 2.5 mL of HCl, 5 mL of HF, and 1 mL of HClO₄ were added. Closed the lid, shook, and left it overnight. Placed the beaker on a hot plate, removed the lid, rinsed with a small amount of water, heated and decomposed at 190 to 210°C, and dried it until the white smoke is exhausted (If the sample was not completely decomposed, HNO₃ and HF was added before evaporating to dry). 5 mL of 50% HCl was added and heated on a hot plate until the solid salts were completely dissolved. The beaker was removed and cooled, and the solution was transferred to a 25 mL polyethylene colorimetric tube, which was supplemented to 25 mL with pure water, and then measured after 4 h.

5. Sample preparation for total sulphur determinations by combustion-IR detection

0.4 g of iron flux was placed in a porcelain crucible, 0.08 g of the sample was placed, The surface of the sample was

covered with 1.5 g tungsten flux. The crucible was placed on the crucible rack of the combustion-IR detection. After the analysis heating was started, the sulfur release curve in the sample was displayed in the data display area of the software.

CONCLUSIONS

In this paper, strategies for overcoming limitations of sulfur determination in geological samples by WD-XRF was developed. When the sample was prepared in the form of beads, sample was diluted to minimize the matrix effect, while the formation of fused glass discs eliminates the influence of the mineral structure. The addition of sulfur-fixing agent can effectively avoid the volatilization loss of sulfur in the sample caused by the high temperature of the fusion process. The sulfur fixation effect of sulfur-fixing agent BaO was better than that of sulfur-fixing agent CaO. The method validation indicated that the addition of BaO can effectively improve the accuracy of the results. Furthermore, with reference to the quality standard assessment proposed by the IGCP, it can be deduced that the method is adequate considering geochemical mapping application. Compared with ICP-OES method and combustion-IR detection method, the WD-XRF method established in this work is an effective method for the determination of sulfur in geological samples.

Acknowledgements. The authors acknowledge financial support from the Project of China Geological Survey (grant number DD20208069).

REFERENCES

1. V. Chubarov, A. Amosova and A. Finkelshtein, *X-Ray Spectrom*, **2016**, *45*, 352-356.
2. B. A. Trust and B. Fry, *Plant Cell Environ.*, **1992**, *15*, 1105-1110.

3. H. Strauss, *Chem. Geol.*, **1999**, *161*, 89-101.
4. G. Norwitz and H. Gordon, *Anal. Chim. Acta*, **1975**, *77*, 239-244.
5. W. Geng, T. Nakajima, H. Takanashi and A. Ohki, *Fuel*, **2008**, *87*, 559-564.
6. S. Andrade, H. H. Ulbrich, V. A. Janasi and M. S. Navarro., *Geostand. Geoanal. Res.*, **2009**, *33*, 337-345.
7. L. P. Bédard, D. Savard and S. J. Barnes, *Geostand. Geoanal. Res.*, **2008**, *32*, 203-208.
8. S. Uhlig, R. Möckel and A. Pleßow, *X-Ray Spectrom.*, **2016**, *45*, 133-137.
9. V. C. Costa, F. A. C. Amorim and D. V. de Babos, *Food Chem.*, **2019**, *273*, 91-98.
10. T.S. Nunes, C. C. Muller, P. Balestrin and A. L. H. Muller, *Anal. Methods.*, **2015**, *7*, 2129-2134.
11. J. S. S. Oliveira, R. S. Picoloto, C. A. Bizzi, P. A. Mello and J. S. Barin, *Talanta*, **2015**, *144*, 1052-1058.
12. S. R. Krzyzaniak, R. F. Santos, F. M. Dalla Nora and S. M. Cruz, *Talanta*, **2016**, *158*, 193-197.
13. K. Shimizu, K. Suzuki, M. Saitoh and U. Konno, *Geochem. J.*, **2015**, *49*, 113-124.
14. A. Smoliński, M. Stempin and N. Howaniec, *Spectrochim. Acta B.*, **2016**, *116*, 63-74.
15. M. Guitouni, *J. Radioanal. Nucl. Chem.*, **2015**, *303*, 1649-1657.
16. G. V. Pashkova, T. S. Aisueva, A. L. Finkelshtein and E. V. Ivanov, *Talanta*, **2016**, *160*, 375-380.
17. M. A. Czerewko, J. C. Cripps, J. M. Reid and C. G. Duffell, *Cement Concrete Comp.*, **2003**, *25*, 657-671.
18. V. Chubarov, A. Amosova and A. Finkelshtein, *X-Ray Spectrom.*, **2016**, *45*, 352-356.
19. P. Bran-Anleu, F. Caruso, T. Wangler, E. Pomjakushina and R. J. Flatt, *Microchem. J.*, **2018**, *141*, 382-387.
20. T. Y. Cherkashina, S. I. Shtel'makh and G. V. Pashkova, *Appl. Radiat. Isot.*, **2017**, *130*, 153-161.
21. W. Zhao, B. Lu, S. Lv, C. Zhou and Y. Yang, *New J. Chem.*, **2020**, *44*, 11224-11230.
22. V. Chubarov, T. Aisueva and A. Finkelshtein, *Anal. Lett.*, **2016**, *49*, 2099-2107.
23. P. Roy, V. Balaram, R. S. Singh, A. K. Krishna, C. D. Chavan, S. N. Charan and N. N. Murthy, *Atom. Spectrosc.*, **2009**, *30*, 178-183.
24. M. F. Gazulla, M. P. Gomez and M. Orduna, *X-Ray Spectrom.*, **2009**, *38*, 3-8.
25. A. K. Krishna, T. C. Khanna and K. R. Mohan, *Spectrochim. Acta B.*, **2016**, *122*, 165-171.
26. A. G. Darnley, A. Bjorklund, B. Bolviken, N. Gustarsson, P. V. Koval, J. V. Plant, A. Streenjelt, M. Tauchid and M. Xuijing, "Final Report of IGCP Project 259", 1995, p. 122.

